Journal of Engineering Physics and Thermophysics, Vol. 74, No. 2, 2001

NUMERICAL ANALYSIS OF THE EFFECT OF VISCOSITY ON THE VORTEX DYNAMICS IN LAMINAR SEPARATED FLOW PAST A DIMPLE ON A PLANE WITH ALLOWANCE FOR ITS ASYMMETRY

S. A. Isaev, A. I. Leont'ev, P. A. Baranov, Kh. T. Metov, and A. E. Usachov

UDC 532.517.2

Based on numerical solution of the Navier–Stokes three-dimensional stationary equations by a factorized finite-volume method, the influence of physical viscosity on self-organizing jet-vortex structures in a dimple on a plane immersed in a laminar flow is analyzed with allowance for the asymmetry of the dimple shape.

1. The generation of self-organizing large-scale vortex structures in flow past a spherical dimple on an exposed surface has long attracted the attention of experimentalists [1–5] and, primarily, in connection with the solution of the fundamental problem of hydrodynamics and thermophysics and, in particular, of the tasks of enhancing heat exchange in the elements of propulsion systems. However, up to the present time the works carried out have lacked system to a certain extent because of the limited possibilities of physical experiments, especially as concerns the evaluation of the effect of geometrical and operational factors. Thus, for example, the difficulties in conducting investigations in the region of moderate Reynolds numbers that corresponds to a laminar mode of flow are well known. This is why great hopes are pinned on the development of the methods of numerical simulation of three-dimensional flow past a dimple on an exposed wall; they make it possible to analyze in detail the vortex structure of the flow and to obtain the dependences of the local and integral characteristics on the governing parameters [6–14].

The genesis of this trend is closely associated with the evolution of computational complexes used to simulate a three-dimensional flow around objects of curvilinear geometry, and it is characterized by additional complexities gradually introduced into the formulation of the problems considered. The common feature of all the complexes is the application of the concept of splitting as to physical processes and of the finite-volume method of approximation of starting Navier–Stokes equations.

In [6, 7], the results of computer visualization of a vortical laminar flow within the neighborhood of the dimple are systematized. The results included also the cases of nonstationary development of the process and flow blocking in a thin layer adjacent to the wall. All of the calculations used the approach which was based on oblique Cartesian grids adapted to a curvilinear wall exposed to a flow. Unfortunately, the authors failed to attain a high resolution of the details of separation flow because of the small (of the order of several thousands) number of computational meshes within the dimple.

The solutions were substantially improved by using a cylindrical grid to map the neighborhood of a spherical dimple [8–11]. The number of computational cells in the region of the laminar separation flow considered was increased here by an order of magnitude and attained several thousands. As a result, the self-or-

Academy of Civil Aviation, St. Petersburg, Russia; email: isaev@SI3612.spb.edu. Translated from Inzhenerno-Fizicheskii Zhurnal, Vol. 74, No. 2, pp. 62–67, March–April, 2001. Original article submitted August 14, 2000.

1062-0125/01/7402-0339$25.00

ganizing large-scale flow-forming structures in the dimple were analyzed in detail; they include swirled jets of tornado type and vortex rings. It is also discovered that the deformation of the dimple shape in a transverse direction leads to rearrangement of the flow pattern from a symmetrical one with two vortical cells in the dimple to an asymmetrical one with predominant liquid transfer across the main flow; this rearrangement is accompanied by enhancement of heat transfer from the wall.

And, finally, the application of a computational strategy based on multiblock intersecting grids made it possible to reach a new level of simulation of flow past a deep dimple [12, 13]; the level combines correct mapping of differently scaled structural elements of a three-dimensional flow with allowance for the effect of turbulence, natural convection, and jamming of flow by channel walls.

It should be noted that the first attempts made abroad to calculate this kind of flow (see, e.g., [14]) are still of limited methodical character and are also distinguished by a simplified formulation of the problem (in particular, in the work cited the effect of an external stream on the flow in a spherical dimple is replaced by motion of the upper boundary).

The present work is a continuation of numerical investigation [13] and is aimed at a detailed analysis of laminar incompressible viscous liquid flow past a dimple on a plane, with particular attention paid to the effect of the asymmetry in the dimple shape on the deformation of the vortical flow. Just as in the above-mentioned work, the three-dimensional jet-vortex structures were identified by the method of computer visualization of flow by observing the tracks of labeled liquid particles. As a base geometry, a spherical dimple (of depth 0.22) with rounded edges (of radius 0.1) is considered, for which a regime of stable flow with the formation of an extended separation zone is realized.

2. In numerical simulation of laminar flow in the vicinity of a curvilinear relief an approach is being developed which was tested in solving two-dimensional flows around bodies with vortex cells and which is based on the use of multiblock grids [12]. The constructed factorized algorithm is based on the implicit finite-volume method of solving the Navier–Stokes equations within the framework of the concept that the computational domain can be decomposed and that in oblique grids of H- and O-type with overlapping can be generated the isolated substantially differently scaled subregions. The system of starting equations is written in a divergent form for increments of dependent variables that involve, in particular, Cartesian velocity components. In approximation of source terms, the convective fluxes are determined with the aid of a one-dimensional countercurrent scheme with quadratic interpolation. The details of the implicit finite-volume computational procedure based on the concept of splitting according to physical processes are given in [6, 7].

Within the framework of the multiblock grid strategy the values between intersecting grids are carried over with the aid of nonconservative linear interpolation. The volume of the mesh of the selected structured grid is divided into six pyramids, whose base is one of the faces and the whose vertex is at the center of the mesh. Each pyramid is divided, in turn, into eight tetrahedrons. The intergrid interpolation determines the relevance of the point selected, at which one has to determine the set of parameters, to one of the tetrahedrons that form the mesh; for this tetrahedron, linear interpolation is constructed from the known values at vertices. Thus, for the tetrahedron with the vertices P_1, P_2, P_3, and P_4, the value of the function F at an arbitrary point P will be written in the form $F_P = \sum_{i=1}^{4} F_i h_i$, where $F_i = F(P_i)$ is the value of the function at the ith vertex of the tetrahedron, while the coefficients of the interpolation dependence are defined by the expression $h_i = \text{vol}\,(P, P_m, P_n, P_h)/\text{vol}\,(P_1, P_2, P_3, P_4)$, where m, n, and k are the numbers of the successive vertices of the tetrahedron (1, 2, 3; 2, 3, 4; 3, 4, 1; 4, 1, 2) and i is the number-complementary vertex (4, 1, 2, and 3, respectively). Here vol (P_1, P_2, P_3, P_4) is the volume of the tetrahedron with the indicated vertices.

3. To solve the problem of laminar flow past a deep dimple and more accurately resolve differently scaled structural elements of flow such as a shear layer and a zone of back flow, it seems worthwhile to isolate, around the dimple, the near-wall region of annular cylindrical shape of outer radius 1 (all the linear

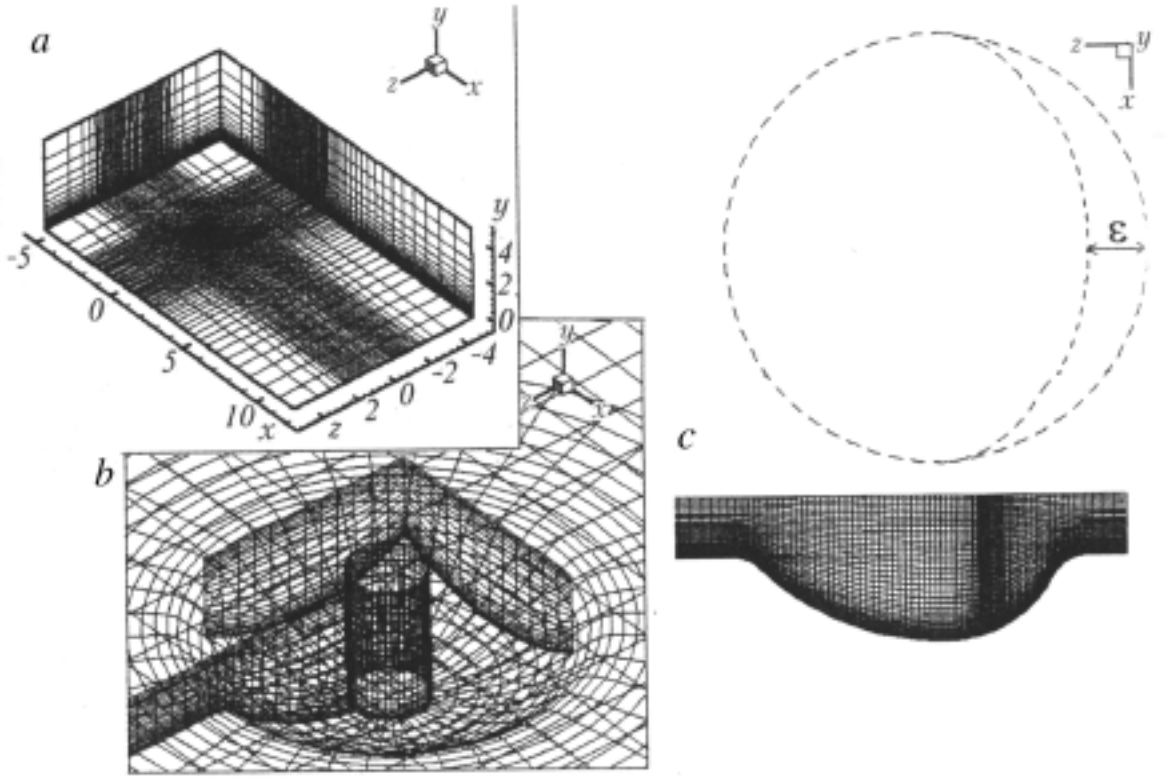

Fig. 1. Computational domain (a), a fragment of a multiblock grid (b) to calculate flow past a spherical dimple of depth 0.22 and curvature radius 0.1, and also the contour of an asymmetric dimple (spherical-elliptic) with the ratio of semiaxes 0.3 to 0.5, and cross section of the dimple at middle (c).

dimensions are related to the diameter of the dimple), inner radius 0.1, and height 0.175. The region considered is divided by an oblique curvilinear grid matched with the exposed surface. Sixty uniformly distributed meshes are selected over the circumference and from 30 to 45 meshes in the vertical direction with the concentration of nodes near the wall (the minimum near-wall step varied from 0.0008 to 0.005). From 30 to 45 meshes are prescribed in the radial direction, with smaller and smaller step size to the boundary of the dimple (the minimum step is 0.006).

The considered subregion of the dimple is overlaid by a large-scale rectangular region whose base partially coincides with the plane wall exposed to the flow (Fig. 1a). The origin of the Cartesian coordinate system coincides with the projection onto the plane of the dimple center. The length of the region is 17, the height 5, and the width 10. The indicated region is divided by the Cartesian grid having $55 \times 35 \times 40$ meshes. The nodes of the grid are concentrated in the vicinity of the dimple (the minimum step in the longitudinal and transverse directions is 0.1) and near the wall (the near-wall step varies from 0.001 to 0.005).

To resolve the wall flow in the vicinity of the axis of the cylindrical subregion in the best way a "patch" intersecting this subregion is introduced (Fig. 1b) that has the shape of a curvilinear parallelepiped. Within the limits of this patch, a grid is constructed with uniform distribution of nodes in the longitudinal and transverse directions. The steps of this grid agree with the near-boundary step of the grid of the neighboring cylindrical region. The disposition of the nodes in the vertical direction is also kept in coordination.

The flow past two types of dimples was analyzed: of spherical shape and of asymmetric geometry, which is a combination of a spherical and an elliptic one (with the ratio of half-axes 0.3 and 0.4 to 0.5) (Fig. 1c). The asymmetry parameter ε changes here from 0.1 to 0.2.

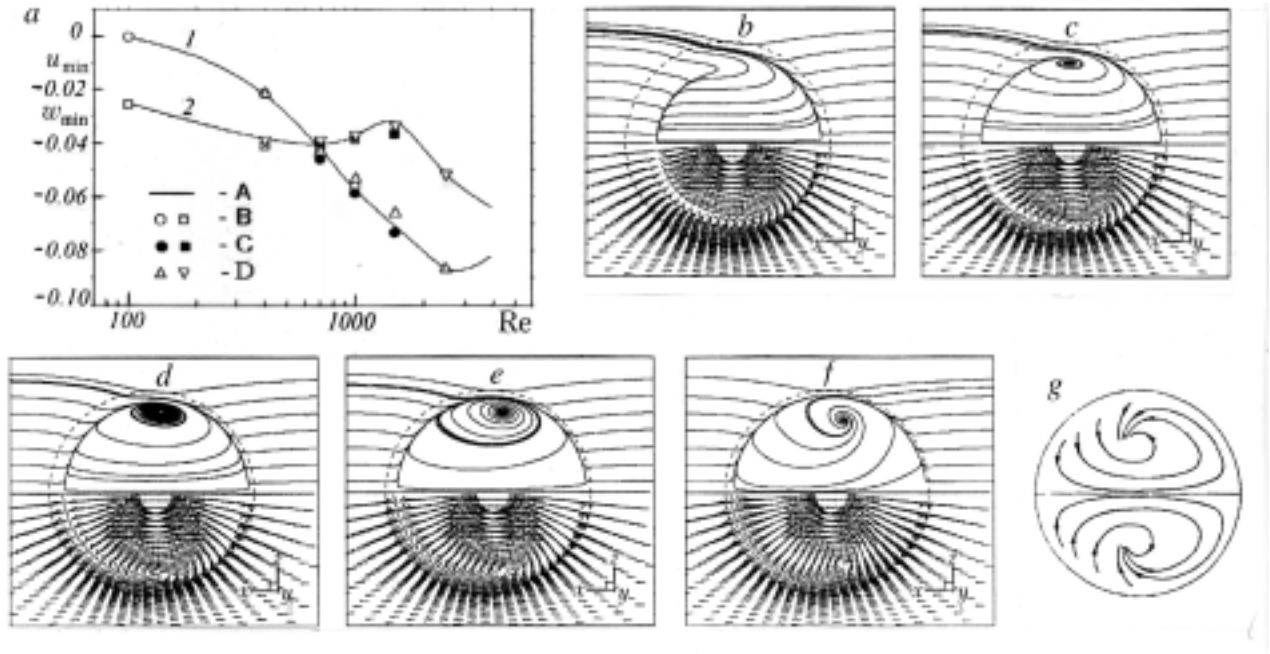

Fig. 2. Dependence of minimum values of the longitudinal (1) and transverse (2) velocity on the Re number (a) for computational grids with different density of meshes and evolution of the patherns of spreading of liquid over the surface of a deep dimple with increase in the Reynolds number: b) Re = $4 \cdot 10^2$; c) $7 \cdot 10^2$; d) 10^3; e) $1.5 \cdot 10^3$; f) $2.5 \cdot 10^3$; g) $2.5 \cdot 10^3$; (experiment [1]). Grid contains 137,700 meshes in the computational domain and 51,300 meshes within the dimple; B – 94,500 and 15,000; C – 220,400 and 103,800; D – 179,232 and 91,232, respectively.

On the inlet boundary of the computational domain (Fig. 1), the velocity profile corresponding to the Pohlhausen profile for a laminar boundary layer is prescribed, with the thickness equal to the depth of the dimple is prescribed. On the outlet boundaries mild boundary conditions are set (the conditions of the continuation of solution from the inner points to the boundary of the region). No-slip conditions hold on the wall. The free stream velocity outside the boundary layer and the dimple diameter, which is taken to be equal to the length of transition from the curved portion to the plane, are taken as the parameters of nondimensionalization.

The Reynolds number varies from 10^2 to $2.5 \cdot 10^3$. The calculations were carried out on several multiblock grids that contained meshes of the order of $(1–2.5) \cdot 10^5$ in the case of nearly coinciding thicknesses of the boundary layer (the range of variation is 0.175–0.22) and a different number of meshes within the limits of the spherical dimple and also when the near-wall step of the grids changed.

4. Some of the results obtained are given in Figs. 2–4 and in Table 1. As in [13], attention is especially paid to computer identification of self-organizing jet-vortex structures that play a dominant role in the physical mechanism of vortical (tornado) intensification of heat and mass exchange processes in flow past reliefs with cavities. Comparison of predicted results with available experimental data is made [1].

Methodical numerical experiments carried out to evaluate the effect of the prescribed number of meshes on the results of calculation (Fig. 2a), especially those disposed within the limits of a spherical dimple, demonstrate weak dependence of the results on grid factors. This indicates the adequacy of the computational complex for simulation of spatial laminar separation flows.

The intensification of a recurrent flow in a dimple with increase in Re is first of all characterized by monotonous increase in the absolute value of the minimum longitudinal velocity component u_{min}. At Re =

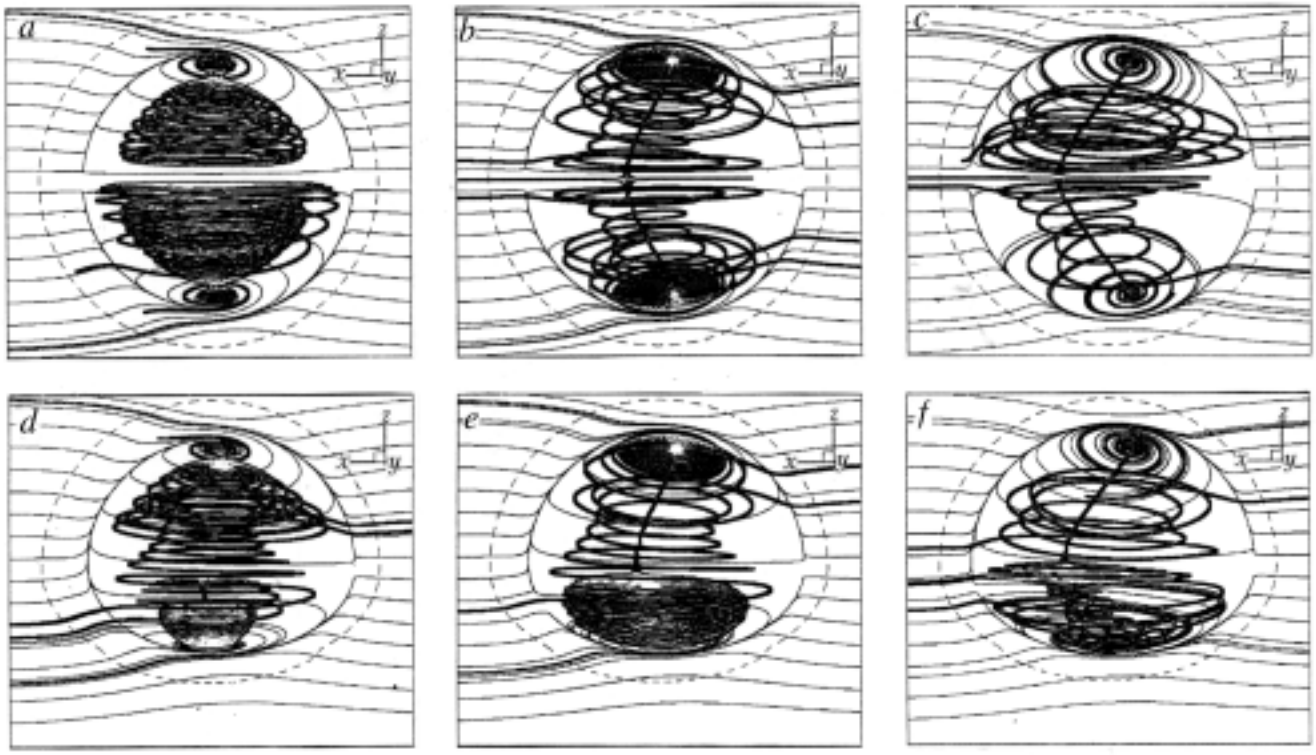

Fig. 3. Pictures of vortex structures in laminar flow past a symmetric (a, b, c) and asymmetric (d, e, f) dimple at Re = $7 \cdot 10^2$ (a, d) and $1.5 \cdot 10^3$ (c, f).

10^2 there is virtually no separation flow in a deep dimple, and at Re = $2.5 \cdot 10^3$ the maximum velocity of the return flow is equal to 9% of the external flow velocity.

As Re increases, the minimum value of the transverse velocity component w_{min} that characterizes the degree of the capturing of liquid by the dimple from the surrounding space (vacuum cleaner effect) behaves abnormally. At low values of Re the absolute value of w_{min} increases, though to a lesser degree than u_{min}, and then at Re of the order of 10^3 it begins to decrease, attaining the local extremum at Re ≈ 1050. Thereafter, as Re increases w_{min} continues to increase, confirming the tendency toward intensification of the separation flow in the dimple. When Re = $2.5 \cdot 10^3$, the quantity w_{min} takes the value −0.052. It should be noted that at low (of the order of 10^2) Reynolds numbers the quantity w_{min} in absolute value comes to 2.5% of the external flow velocity.

It is seen from Fig. 2b-d that as the Re number increases, the evolution of the pictures of liquid spreading over the surface of a deep spherical dimple, with the radius of curvature of the sharp edge equal to 0.1, demonstrates transition from a quasi-two-dimensional character of separation flow at low (10^2–$4 \cdot 10^2$) Reynolds numbers to a flow regime with the formation of special focus-type points (Fig. 2c, d). As Re increases, the dimensions of the separation region of flow become larger, and the separation line comes nearer to the front boundary of the dimple shown in Fig. 2 by the dashed line. Here, it is important to emphasize that at low Re the motion of liquid along the line of flow attachment is directed from the longitudinal plane of symmetry of the dimple to its periphery and vice versa at moderate and high (above $7 \cdot 10^2$) Reynolds numbers.

It is of interest to analyze the structure of wall flow developed on the side slopes of the dimple. At low and moderate Re numbers (up to 10^3) specific windows are formed, through which the liquid, if trapped, escapes from the dimple. However, while at low values of Re the flow at the periphery of the dimple turns smoothly, at higher values of Re the change in the direction of liquid motion along the line of flow attachment first determines the local and then global (in the scale of the dimple) swirl of the flow. With increase

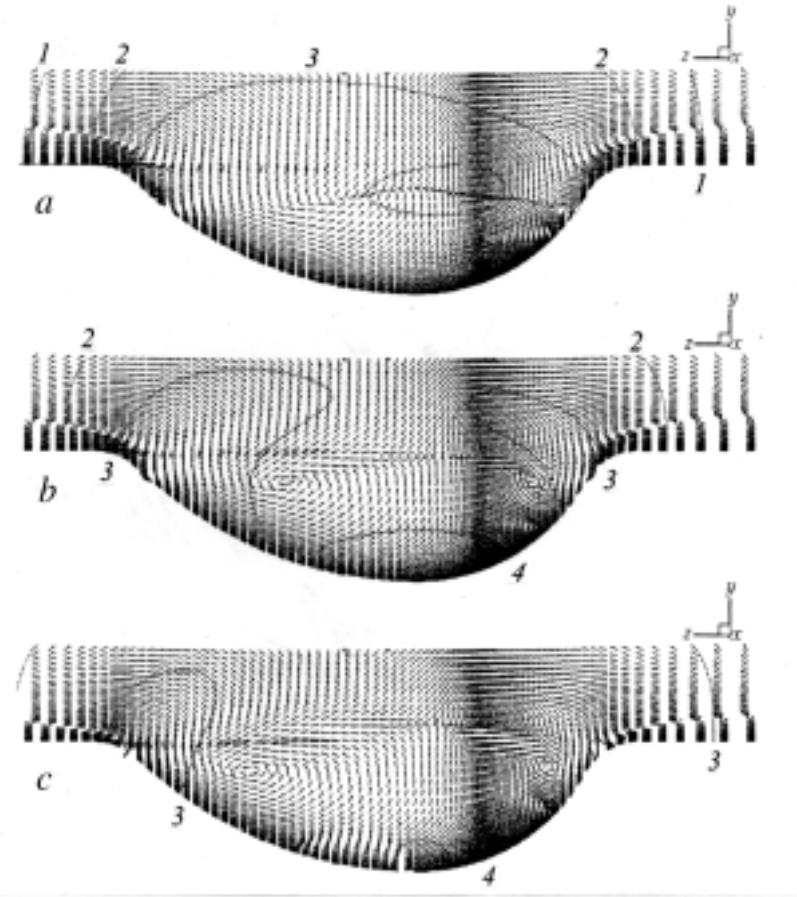

Fig. 4. Evolution of the secondary flow in the transverse median plane of an asymmetric dimple at the half-axes ratio 0.3 and 0.5 with increase in the Reynolds number: a) Re = $7 \cdot 10^2$; b) 10^3; c) $1.5 \cdot 10^3$. The dashed lines show isobars (the pressure p is related to doubled velocity head): 1) p = 0; 2) 0.002; 3) 0.004; 4) 0.006.

in the Reynolds numbers, the flow area of the windows is reduced till the separation zone is closed at Re $\approx 1.5 \cdot 10^3$. It should be noted that the closure of the separation zone corresponds to the extremum of the function $w_{\min}(\mathrm{Re})$. Thereafter, the separation region opens to meet the incoming flow, as a result of which the small jets of the stream directly enter the dimple through the side windows, increasing the circulation of vortex flow in it.

On the whole, the distinct three-dimensional effects typical of flow past a deep dimple begin to manifest themselves already at moderate Reynolds numbers, when the separation flow loses its quasi-two-dimensional nature in the central part of the dimple and the sinks on its side walls are being formed. At large Reynolds numbers (of the order of $2.5 \cdot 10^3$), two large-scale vortical cells are formed that are located symmetrically relative to the median longitudinal plane of the flow. Rotational motion of liquid relative to the foci is developed in them. With increase in Re, a tendency toward the motion of the indicated points to the center of the dimple is observed. The calculated picture of the spread of liquid in the wall layer of the dimple correlates satisfactorily with the experimentally observed stationary flow in a dimple at nearly the same Reynolds number [1] (Fig. 2j).

The visualization of stream-forming structural elements in a laminar separation flow past a dimple reveals (see Fig. 3) that the rearrangement of the vortex structure in transition from moderate to high Reynolds numbers is associated with the formation of jet-like tornado-type flows emerging from the neigh-

TABLE 1. Hydrodynamic Resistance and Its Components of the Circular (radius 1) Element of the Wall with the Dimple at Re = 10^3

Type of surface	C_{xp}	C_{xf}	C_x
Smooth wall	–	0.02514	0.02514
Spherical dimple	0.00469	0.01743	0.02212
Asymmetric dimple	0.00445	0.01762	0.02207
Asymmetric dimple with $\varepsilon = 0.2$	0.00388	0.01756	0.02144

borhood of the foci on the surface of the dimple. At Re = $7 \cdot 10^2$ the indicated peripheral flows are still very weak, and on the whole jamming of the closed vortex flow in the central region of the dimple is observed, with the enclosing of it by the near-wall layers of the swirled flow. The liquid from the center of the dimple is carried away to the periphery and is expelled from it, in particular, through the side windows.

When Re > 10^3, the liquid from the peripheral side regions moves to the center and subsequently is swept out of the symmetry plane. As already noted in [11], the axes of the swirled jets at high Re numbers are straight lines that connect the foci on the walls of the dimple with the sink point in the middle longitudinal plane around which rotational motion of liquid particles originates in the plane of symmetry. The trajectories of liquid particles that enter into the dimple from the outer flow are coiled round the axes of the jets. The particles from the peripheral portion of the dimple are transferred along the small radii. As seen from Fig. 3b, the liquid particles that belong to the external flow and that enter into the central part of the dimple are entrained into the core of the swirled jet flow near its base. Consequently, the liquid from the central part of the dimple is transported to its periphery along the trajectories with decrease in the radius of swirling.

For an asymmetric dimple produced by deformation of the side wall so that, when viewed from above, its edge has an elliptic shape, the flow acquires an asymmetric character. As seen from Fig. 3d-f, a predominant transfer of liquid from the hemispherical part of the dimple into its deformed part is observed. However, this is not caused by a substantial increase in convective transfer in the hemispherical portion; on the contrary, the motion of liquid in this part of the dimple is similar to flow past a spherical dimple. Rather, one should speak about the weakening of vortical flow in the deformed part of the dimple. As shown in [13], this tendency in a turbulent regime leads to cardinal rearrangement of the regime of flow in the dimple due to the transition from the structure with two vortex cells to a monovortex tornado-like structure. As a result, there is not only intensification of the secondary flow in the asymmetric dimple but also a considerable enhancement in heat exchange of the surface element having such a dimple.

In laminar flow past an asymmetric spherically elliptic dimple, just as in the case of a deformed round dimple with a variable curvature radius [8, 10, 11], an interference of swirled jet flows of different intensity is noted within its bounds. Figure 3d, e distinctly shows the interface between the interacting flows that block the vortex cell on the deformed side of the dimple.

It is of interest to analyze the evolution of the pattern of secondary flow in the middle cross section of the asymmetric ($\varepsilon = 0.2$) dimple on increase in the Reynolds number from $7 \cdot 10^2$ to $1.5 \cdot 10^3$ (Fig. 4).

The common features of the pattens given are the outflow of liquid from the dimple on its sides and ejection of liquid from the external flow into the dimple. The entrainment of liquid from the side of the spherical part turns out to be predominant. It forms a strong transverse flow in the dimple in the direction of its deformed part; the flow becomes stronger as Re increases. At Re = $7 \cdot 10^2$ this flow cannot withstand the zone of higher pressure, ascends, and, interacting with the descending external flow that comes from the right, it spreads in the longitudinal plane on the interface between the streams and forms a high-pressure region (Fig. 4a), When Re ≥ 10^3, two spiral-like vortical rings are formed as a result of interaction of the ascending and descending streams. As the Reynolds number increases, the zone occupied by the vortices be-

comes larger and larger, and the interface between the streams rises over the plane. A tendency toward equalization of pressure in the cross section of the dimple is noted.

And, finally, we will compare the tabulated integral force characteristics that influence the circular element of a smooth wall of unit radius in the presence and absence of a dimple. It is important to emphasize that the presence of a spherical dimple leads to a substantial, 30%, drop in the friction resistance C_{xf}. Of course, a pressure resistance C_{xp} appears in this case that comes to about 19% of the resistance of the plane element. Nevertheless, the total resistance of the circular element with the considered spherical dimple C_x turns out to be approximately 11% lower than the friction resistance of the plane element. The use of asymmetric dimples favors a decrease in the profile resistance and practically does not influence the friction resistance. Thus, the total resistance of the circular element with an asymmetric dimple at $\varepsilon = 0.2$ can be reduced by 15% in comparison with the case of a plane wall.

This work was carried out with financial support from the Russian Foundation for Basic Research, project Nos. 00-02-81045, 99-01-00722, and 99-02-16745.

REFERENCES

1. P. R. Gromov, A. B. Zobnin, M. I. Rabinovich, et al., *Pis'ma Zh. Tekh. Fiz.*, **12**, Issue 21, 1323–1328 (1986).
2. V. N. Afanas'ev, V. Yu. Veselkin, A. I. Leont'ev, et al., *Hydrodynamics and Heat Exchange in Flow Past Single Depressions on an Originally Smooth Surface*, Preprint No. 2-91, Pts. 1, 2, N. É. Bauman Moscow State Technological University [in Russian], Moscow (1991).
3. Yu. M. Mshvidobadze, *Aerodynamics and Heat Exchange in a Spherical Cavity*, Candidate's Dissertation in Technical Sciences, Novosibirsk (1997).
4. V. V. Alekseev, I. A. Gachechiladze, G. I. Kiknadze, et al., in: *Proc. 2nd Russ. Nat. Conf. on Heat Exchange*, Vol. 6, *Enhancement of Heat Exchange. Radiative and Combined Heat Exchange* [in Russian], Moscow (1998), pp. 33–42.
5. N. Syred, A. Khalatov, A. Kozlov, et al., *ASME Paper*, No. 2000-GT-236 (2000).
6. S. A. Isaev, A. I. Leont'ev, and A. E. Usachov, *Izv. Ross. Akad. Nauk, Énergetika*, No. 4, 140–148 (1996).
7. S. A. Isaev, A. I. Leont'ev, and A. E. Usachov, *Inzh.-Fiz. Zh.*, **71**, No. 3, 484–490 (1998).
8. S. A. Isaev, A. I. Leont'ev, A. E. Usachov, et. al, *Numerical Simulation of Laminar Three-Dimensional Viscous Incompressible Liquid Flow Past a Dimple (Vortical Dynamics and Heat Exchange)*, Preprint No. 6–99, Institute of Highly Efficient Computations and Data Bases [in Russian], St. Petersburg (1997).
9. S. A. Isaev, A. I. Leont'ev, A. E. Usachov, et al., *Pis'ma Zh. Tekh. Fiz.*, No. 6, Issue 24, 6–10 (1998).
10. S. A. Isaev, A. I. Leont'ev, A. E. Usachov, et al., in: *Proc. 2nd Russ. Nat. Conf. on Heat Exchange*, Vol. 6, *Enhancement of Heat Exchange. Radiative and Combined Heat Exchange* [in Russian], Moscow (1998), pp. 121–124.
11. S. A. Isaev, A. I. Leont'ev, A. E. Usachov, et al., in: *Izv. Ross. Akad. Nauk, Énergetika*, No. 2, 126–136 (1999).
12. S. A. Isaev, in: *Proc. 12th School-Seminar of Young Scientists and Specialists under the Leadership of A. I. Leont'ev, Academician of the Russian Academy of Sciences "Problems of Gasdynamic and Heat and Mass Exchange in Power Plants"* [in Russian], Moscow (1999), pp. 17–20.
13. S. A. Isaev, A. I. Leont'ev, P. A Baranov, et al. in: *Proc. 4th Minsk Int. Forum on Heat and Mass Transfer*, Vol. 1, *Convective Heat and Mass Transfer* [in Russian], Minsk, May 22–26, 2000, Minsk (2000), pp. 507–514.
14. M.-H. Chang and C.-H. Cheng, *Int. Comm. Heat Mass Transfer*, **26**, No. 6, 829–838 (1999).